ACS APPLIED MATERIALS & INTERFACES

Research Article

www.acsami.org

Micro/Nano-Structured Polypyrrole Surfaces on Oxidizable Metals as Smart Electroswitchable Coatings

Luis Santos, Pascal Martin, Jalal Ghilane, Pierre Camille Lacaze, and Jean-Christophe Lacroix*

NanoElectroChemistry Group, ITODYS, UMR 7086 CNRS, Université Paris Diderot, Sorbonne Paris Cité, 15 rue Jean-Antoine de Baïf, 75205 Paris Cedex 13, France

Supporting Information

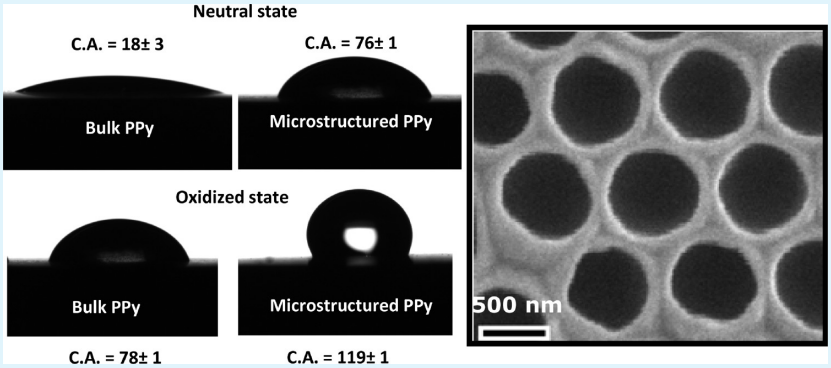

ABSTRACT: Polypyrrole (PPy) films were electrodeposited from a pyrrole/sodium salicylate solution in water, through two-dimensional (2-D) polystyrene (PS) templates self-assembled on various oxidizable metals, after which the template was removed by dissolution in tetrahydrofuran (THF). The resulting PPy films were analyzed by scanning electron microscopy and atomic force microscopy. Two-dimensional PPy honeycomb structures are obtained on copper or mild steel by using PS spheres of various sizes. The morphology of these structures was controlled electrochemically, as an increase in the polymerization charge does not disturb the PPy honeycomb arrangement, leading instead to the formation of deeper pores accompanied by a change in their diameter. The hydrophobicity of the reduced micro-structured PPy surface is much greater than that of a bulk PPy film generated on the same metal. Reversible electro-switching of the wettability was obtained with marked variation of the apparent contact angle upon PPy oxido-reduction, and an important effect of film micro-structuration upon the wettability range.

KEYWORDS: *conducting polymer, nanosphere lithography, electrodeposition, anticorrosion, switchable hydrophobicity*

INTRODUCTION

Conducting polymers (CPs) have been extensively studied over the past 30 years in view of their potential application as molecular[1−3] plastic electronic devices,[4,5] biosensors,[6] and smart surfaces.[7−9] They have been proposed and used as anti-corrosion coatings[10,11] for metals such as copper,[12] zinc,[13] and iron.[14] The various mechanisms of protection against corrosion in which CPs are involved have been recently reviewed.[15,16] In one of them, the CP can act as an insulating layer and physically blocks the access of solvent and oxygen to the underlying metal.[16] In the specific case of polypyrrole (PPy), protective coatings on iron/steel,[17−19] copper,[12,20] Zn,[13] as well as on CuZn,[21] and Al[22] alloys have been reported.

Polymer micro/nano-structuration plays an important role in improving the performance or in extending the functionalities of CP systems.[23] Micro/nano-structured CPs can be synthesized through chemical[24] or electrochemical routes. Electropolymerization allows better control of the quality of the micro/nano-structured materials obtained (by adjusting the electrochemical parameters) and is a powerful means for easy production, in a one-step process, of a multitude of nano- and micro-objects (nano-wires, micro-containers, cups, goblets, and so on).[25] Notwithstanding the progress towards the generation of nano-structured CPs in a single electrochemical step,[26] the use of templates, easily removable after polymer formation, is still very popular. A simple approach towards the electrochemical synthesis of ordered micro-porous/nano-porous CPs is to electro-polymerize monomers within the interstitial spaces between closely packed colloidal templates, which are subsequently removed by using appropriate solvents. Nanosphere lithography (NSL) is the most commonly used technique for this purpose. NSL is a simple, low-cost technique, known to produce ordered patterns for the subsequent fabrication of structured devices of variable size.[27] Sumida et al.[28] were the first to report the preparation of macro-porous PPy films electrochemically using NSL on F-doped SnO_2-coated glasses. Shortly afterwards, Bartlett et al.[29] described a general approach for the synthesis of highly ordered macro-

Received: July 16, 2013
Accepted: September 24, 2013
Published: September 24, 2013

porous conducting films of PPy, polyaniline, and polybithiophene on gold. More recently, micro/nano-structured poly(ethylene dioxythiophene) (PEDOT)[30] and even ultrathin nano-structured organic layers generated through the reduction of diazonium salts[31] have been produced via NSL on glassy carbon, indium tin oxide (ITO), and noble metals. NSL was used for the electrochemical preparation of nano-porous/inverse opal CP structures with potential biosensing applications on gold,[32−35] glassy carbon,[36] and platinum.[37] It was also employed to electro-synthesize macro-porous/mesoporous CPs on transparent semi-conductors to generate optoelectronic devices like photonic crystals,[38] organic light-emitting diodes (OLED),[39] and solar cells.[40,41]

NSL is also a convenient way of achieving high surface roughness, which enhances the hydrophobicity of the CP film, as was demonstrated by Xu et al. who successfully fabricated PPy inverse opals with switchable wettability on an ITO-coated glass substrate.[42] As a consequence, it was proposed that the enhancement of the hydrophobicity of CP structured layers could lead to an improvement of their anti-fouling or corrosion-protective properties when deposited on coinage metals. Indeed, increased hydrophobicity is very desirable in corrosion protection since it prevents water from being absorbed onto the coating and corrosive chemicals from diffusing through the coating. However, to the best of our knowledge, reports on the corrosion protection studies associated with highly or superhydrophobic surfaces using electroactive polymer coatings are limited[8,43] even though a few reports, using nanocasting techniques for CP deposition, have appeared recently.[43] In this context, the micro-structuration of CPs on oxidizable metals via monomer electro-polymerization within the interstitial spaces between closely packed colloidal templates has not been the subject of much attention, and it is only recently that a first paper describing superhydrophobic colloidally textured, but poorly ordered, polythiophene, films as superior anti-corrosion coatings on stainless steel were reported.[44]

Here we report a simple, reproducible method for preparing well ordered, two-dimensional (2-D) PPy honeycomb structures on several oxidizable metals (copper and mild steel) using NSL. Close-packed colloidal PS nanospheres were employed as a template, and pyrrole was electropolymerized from an aqueous solution of pyrrole/sodium salicylate (SS) within the interstitial voids of the PS assemblies. The PS nanospheres were then dissolved by immersion of the modified electrode in tetrahydrofuran (THF). The modified surfaces were characterized electrochemically, and their morphology analyzed by atomic force microscopy (AFM) and scanning electron microscopy (SEM). Easy control of the nanopore separation and diameter is achieved by employing PS spheres of various sizes. Finally, the dynamic wettability of a micro-structured PPy electrodeposited on a mild steel surface was investigated, and compared to that of a bulk PPy film prepared under similar conditions.

EXPERIMENTAL SECTION

Commercially available reagents were used as received unless otherwise stated. Pyrrole (Bayer) was distilled before use. Lithium perchlorate was purchased from Fluka. Sodium salicylate (SS) was supplied by Sigma. The monodisperse, carboxylate-modified PS spheres with diameters of 250 and 900 nm were obtained from Sigma-Aldrich as 10 wt % suspensions in water.

Self-Assembled Colloidal Template Synthesis. Mild steel and copper substrates were used as substrates for PS template deposition. The substrates were first polished with 5, 1, and 0.05 μm alumina, ultrasonicated in analytical grade acetone for 5 min and dried under N_2. The PS template was then prepared using the vertical deposition method, that is, the suspension of PS spheres in water (dia. = 250 or 900 nm) was diluted to 0.5 wt.% and a 5 μL drop was deposited on the metal surface and allowed to dry. Finally the substrates were heated to 60 °C for 2 h. Before use as working electrode, a precise area (12 mm^2) was delimited on the substrate using insulating paste.

Electrochemical Experiments. Electrochemical experiments were carried out in a single-compartment three-electrode cell using a CHI 660 potentiostat (CH Instruments). The auxiliary electrode was a platinum grid, and a saturated calomel electrode (SCE) (3 M KCl), was used as reference. Py polymerization was carried out from a 0.5 mol L^{-1} monomer/1 mol L^{-1} SS solution, by sweeping the potential between 0 and 0.8 V vs SCE at a scan rate of 0.05 V s^{-1}. After electrochemical deposition of PPy, the PS template was removed by soaking the modified substrates in THF for 48 h.

AFM and SEM Experiments. All AFM experiments were carried out in tapping mode with a Pico plus (Molecular Imaging) at room temperature. The Si cantilevers (NCH Scientec) have an average stiffness, as given by the manufacturer, of about 50 N m^{-1}, and a resonance frequency around 300 kHz. The SEM experiments were performed with a Zeiss Supra 40 in a 10^{-8} Torr vacuum and at an accelerating voltage of 15 kV.

RESULTS AND DISCUSSION

Electrosynthesis of Well-Organized Nano-Structured Films of PPy on Copper and Steel. The 2-D PS template was prepared via a standard procedure using PS spheres bearing hydrophilic shells. Suspensions of different sized beads were tested, and conditions were optimized to obtain on the metal surface a hexagonal close-packed monolayer of PS beads, on which to electrodeposit PPy, as shown in Figure 1.

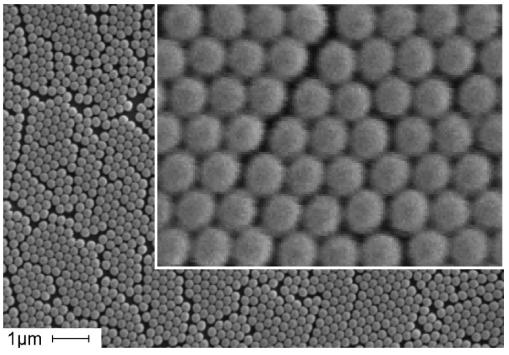

Figure 1. SEM images of an array of PS latex particles (dia. 250 nm) deposited on a copper surface. **Inset**: zoom of the surface.

The cyclic voltammograms (CVs) corresponding to Py polymerization on a 250 nm PS colloidal template deposited on copper, as well as the corresponding characterization after PPy deposition, are presented in Figure 2 and Supporting Information, Figure SI1, respectively. In spite of the very large gap between the pyrrole and the metal oxidation potentials, which thermodynamically should lead to metal dissolution and not to polymer formation, PPy films were formed as easily as on a platinum electrode. This result is explained by the fact that a very thin (around 15 nm), passivating, composite copper salicylate layer ($ZnSac_2$), formed prior to pyrrole electro-polymerization, prevents metal dissolution without inhibiting polymer formation.[20] Note that

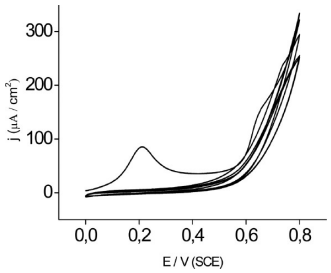

Figure 2. CVs in 0.5M Py/1M SS aqueous solution for a copper surface modified with a template of 250 nm PS nanospheres. ν = 50 mV s^{-1}.

PPy deposition using salicylate solution is a very efficient process already used on various metals.[8,10a,45]

In the present case, shown in Figure 2, the anodic peak at 0.2 V on the first scan (disappearing upon further cycling) is associated with the oxidation of Cu and Cu_2O to soluble copper(II) species and the formation of an ultrathin layer of surface species such as copper salicylate.[20,46] This layer inhibits copper dissolution but still allows the oxidation of Py and subsequent polymerization.[20,47] Indeed, the presence of an oxidation current, near 0.6 V, in all the CVs of Figure 2, can be attributed to Py oxidation and consequent PPy deposition on the copper surface available at the interstitial voids of the colloidal template. This clearly indicates that the presence of the PS particles does not perturb PPy deposition on the copper electrode. Furthermore, as can be seen from the CVs corresponding to the characterization of the PPy/PS/Cu surface (Figure 2 and Supporting Information, Figure SI1), the copper salicylate layer and the PPy film formed at the PS/Cu surface protects the copper from further dissolution, that is, the peak attributed to copper oxidation is absent once PPy has been deposited on the surface in the first cycle.

Figure 3 shows the SEM and the AFM analysis carried on the PPy/Cu surfaces after dissolution of the PS nanospheres. Ten polarization cycles performed on a modified PS/Cu surface, in a Py/SS aqueous solution, generate, after dissolution of the nanospheres, a thin well-defined PPy honeycomb structure displaying pores 100 nm deep and a grating corresponding to the diameter of the PS sphere used. If the polymerization charge is decreased, a thinner PPy membrane, about 35 nm thick, is formed at the copper surface (not shown). These results suggest that well organized 2-D honeycomb PPy films on copper can be synthesized via NSL, allowing the generation of PPy structures with controllable grating size and thickness. Furthermore, the honeycomb structures generated present a good adhesion, since no loss of PPy is observed after electrochemical characterization and after exposing the substrate to THF.

We have investigated the feasibility of this procedure on copper, when larger PS beads are used to change the grating of the micro-structured PPy generated. Figure 4 shows SEM images of a Cu/PS surface, prepared using a 900 nm PS bead template, and modified with 10 (Figure 4a) and 20 (Figure 4b) polymerization cycles, followed by dissolution of the PS particles. The images show that a PPy coating displaying an ordered array of about 900 nm equidistant pores with walls 270 nm thick can be generated on a copper surface when 10 potential cycles are applied at the Cu/PS-modified electrode. Furthermore, the thickness and pore size of the polymer film can be adjusted by the charge (i.e., number of cycles) used during the electrodeposition: as can be observed in Figure 4b, increasing the polymerization charge leads to a reduction of the honeycomb wall width of about 100 nm, as a consequence of an increase in the PPy thickness, which has not yet exceeded the radius of the PS spheres.

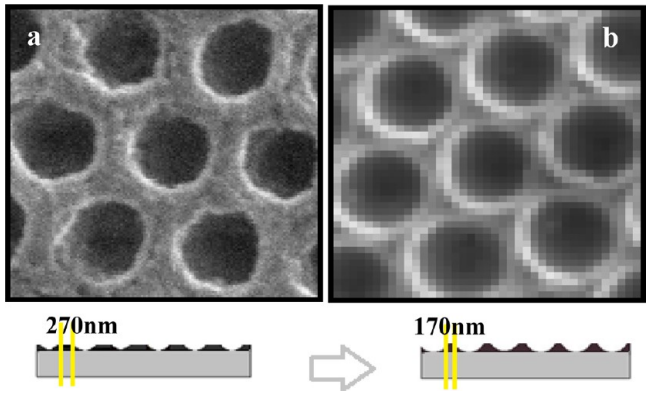

Figure 4. Scanning electron micrographs of a PPy honeycomb film generated by electro-polymerization of Py: (a) 10 cycles and (b) 20 cycles (and schemes corresponding to the film modification) from a solution of 0.5 M Py/1 M SS, in the interstitial voids of a copper surface covered with a close-packed PS particle (dia. 900 nm), followed by dissolution. Cycling is performed between −0.2 and 0.8 V (SCE) at 50 mV s^{-1}.

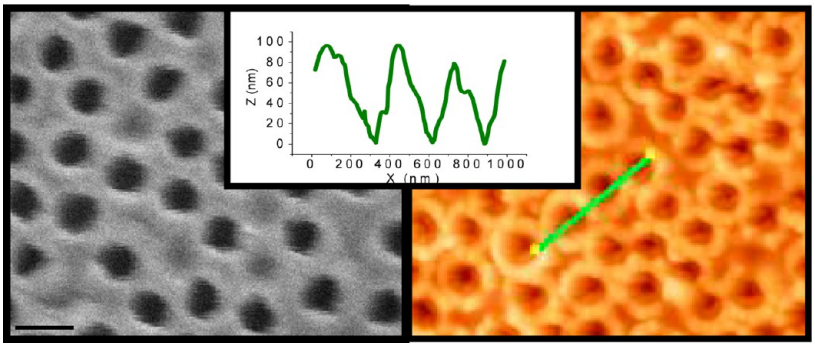

Figure 3. SEM (left), topographic AFM (right) images and cross sections (center) through pores of PPy honeycomb films generated by Py electro-polymerization using 10 polarization cycles from a solution of 0.5M Py/1M SS, in the interstitial voids of a copper surface covered with a close-packed PS particle (dia. 250 nm) followed by dissolution.

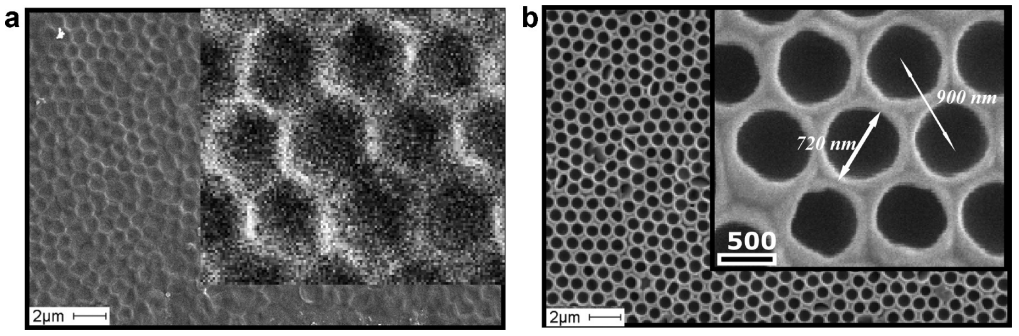

Figure 5. Scanning electron micrographs of a PPy honeycomb film generated by electro-polymerization of Py: (a) 10 cycles and (b) 40 cycles from a solution of 0.5 M Py/1 M SS, in the interstitial voids of a mild steel surface covered with a close-packed PS particle (dia. 900 nm), followed by dissolution. Cycling is performed between −0.2 and 0.8 V (SCE) at 50 mV s^{-1}.

Many oxidizable metal surfaces can be nano-structured using NSL and PPy deposition in aqueous salicylate solution. In the case of steel, honeycomb-structured surfaces can be obtained. Figure 5 shows steel surfaces modified with PPy structures of various thicknesses deposited potentio-dynamically from an aqueous solution of Py/SS through a monolayer of 900 nm PS nanospheres, after dissolution of the PS nanospheres. In Figure 5a the amount of polymer formed between the template is not enough to generate a PPy microporous film after dissolution of the PS beads, it being just possible to observe the fingerprints of the beads on the steel surface. An increase in the polymerization charge makes it possible to generate a nice PPy honeycomb structure leading to a thicker microporous polymer film and, therefore, to an increase in the pore depth. Indeed, a well-defined PPy film is formed at the steel surface displaying an array of 900 nm equidistant micropores nearly 720 nm in diameter separated by 180 nm-wide PPy walls. An intermediate polymerization charge leads to a decrease in the pore diameter along with an increase in wall width from 180 to 210 nm, suggesting that the thickness of the film prepared under these conditions is again less than the radius of the PS spheres. In addition, and despite a few defects, the SEM images show that such nano-structured surfaces can be generated on a relatively large scale.

Electro-Wettability Measurements. One of the important properties of nano/micro-structures is that they may display very interesting hydrophobic properties.[48,49] Abdelsalam et al.[50] have studied the wetting properties of honeycomb-structured gold surfaces formed by electrodeposition of gold through a sub-micrometer template, and have concluded that when the film thickness increases up to the radius of the cavities, the apparent contact angle (CA) for water on the surface increases from 70° (on the flat surface) to more than 130°. Further thickness increase above the radius of the pores provokes a decrease in wettability back to 70°.

The wettability of a highly organized PPy structure generated on steel via NSL was thus evaluated and compared with that of a bulk PPy film grown on the same substrate and under the same conditions. Figure 6a compares the apparent CA of bulk and microstructure PPy substrates in their reduced states (i.e., after polarization below the threshold reduction potential of the PPy film). The roughness of the honeycomb structure changes the hydrophobic/hydrophilic properties of the surfaces drastically. Indeed, the apparent CA increases from about 18° to 76° as a result of micro-structuration. This result confirms those obtained by Abdelasam et al.,[50] and both are in agreement with the theories of Wenzel[48] and Cassie.[49]

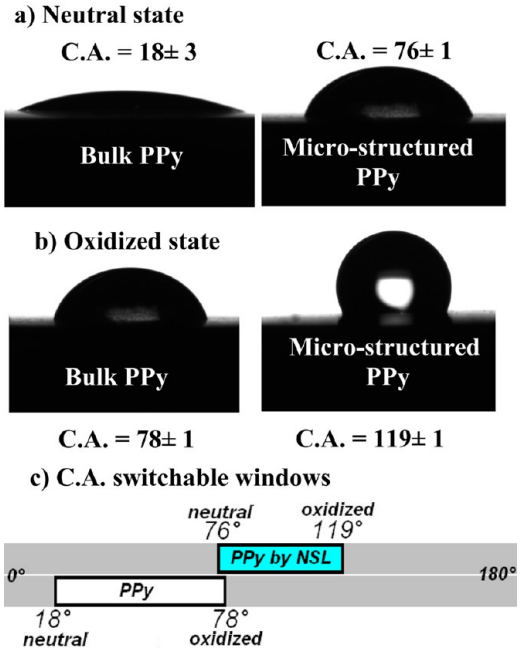

Figure 6. Profile of a water drop on a compact (right) and on a micro-structured (left) PPy film electro-synthesized on steel from a 0.5 M Py/1 M SS solution in water: (a) neutral state ($E_{appl.}$ = −0.85 V/SCE); (b) oxidized state; (c) comparative scheme of the electroactive wettability of a bulk PPy film and a structured PPy film generated via NSL on steel from a sodium salicylate solution, as a function of its redox state.

Furthermore, PPy and polyaniline coatings deposited on noble metals have been proposed as smart surfaces with reversible switchable wettability.[7,9] As these PPy films remain electroactive (see Supporting Information files for CV response of PPy films on mild steel), and since they passivate and protect the underlying metal against corrosion, it is still possible to switch these PPy coatings between their reduced and oxidized states, despite the fact that they are deposited on mild steel. Figure 6b shows the apparent CAs on bulk and micro-structured oxidized PPy films. Bulk PPy film shows hydrophobicity in the oxidation state (ca. 78°) whereas this film is hydrophilic (ca. 18°) in the neutral state. The explanation for this lies in the immobilization of the large salicylate ion in the polymer matrix, which promotes the migration of the hydrophilic Na^+ into the film during the reduction process prior to salicylate ion release.[51,13b] This explains the change in the PPy wettability, from hydrophobic to hydrophilic, ongoing

from the oxidized to the neutral state. In this way, it is thus possible to adjust the wettability of the bulk PPY coating through the potential applied to the surface.

Micro-structured PPy surfaces follow the same trend with a marked increase in the apparent CA upon oxidation of the electroactive polymer. As a consequence, the apparent CA switches from 76° to 119° upon PPy oxidation, and the PPy/steel substrate develops a marked hydrophobic character when combining the highly organized honeycomb structure with the oxidized state of the PPy deposited on the steel surface.

Figure 6c summarizes the CA variations observed upon PPy switching, and it is interesting to note that the two windows of potential-dependent CAs only overlap in the 76−78° region where bulk oxidized PPy and micro-structured reduced PPy have similar apparent CAs. To the best of our knowledge, these results are the first to show that the wettability of CPs can still be profoundly affected by their morphologies and doping states, despite the fact that they are deposited on oxidizable metals.

■ CONCLUSIONS

We have shown that NSL can be used to generate highly organized microporous electroactive PPy films on oxidizable metals, namely, copper and mild steel. Self-assembled PS spheres (dia. = 250 and 900 nm) were employed as templates, and the PPy was deposited under potentio-dynamic control from an aqueous Py/SS solution. The polymer morphology, analyzed by AFM and SEM, is that of 2-D honeycomb-type structures. The morphology can be controlled electrochemically, since an increase in the polymerization charge does not disturb the PPy honeycomb arrangement, leading instead to the formation of deeper pores along with a variation of their diameters. A drastic increase in the hydrophobicity was observed on the reduced micro-structured PPy surface, compared to bulk PPy film generated under the same conditions. Finally dynamic electro-switching of the wettability was obtained, and the apparent CA can be tuned through the combination of PPy micro-stucturation and electrochemical switching.

These highly organized PPy nano/micro-structures, obtained here for the first time on oxidizable metals using NSL, open a new route for the development of smart surfaces based on CPs.

■ ASSOCIATED CONTENT

Supporting Information

Electrochemical characterizations of the PPY coatings. This material is available free of charge via the Internet at http://pubs.acs.org.

■ AUTHOR INFORMATION

Corresponding Author

*E-mail: lacroix@univ-paris-diderot.fr.

Notes

The authors declare no competing financial interest.

■ ACKNOWLEDGMENTS

This work was supported by the CNRS. We are particularly grateful to Dr J. S. Lomas for correcting the English.

■ REFERENCES

(1) Joachim, C.; Gimzewski, J. K.; Aviram, A. *Nature* **2000**, *408*, 541−548.
(2) Chen, F.; Tao, N. J. *Acc. Chem. Res.* **2009**, *42*, 429−438.
(3) (a) Mangeney, C.; Lacroix, J.-C.; Chane-Ching, K. I.; Jouini, M.; Villain, F.; Ammar, S.; Jouini, M.; Lacaze, P.-C. *Chem.—Eur. J.* **2001**, *7*, 5029−5040. (b) Martin, P.; Della Rocca, M. L.; Anthore, A.; Lafarge, P.; Lacroix, J. C. *J. Am. Chem. Soc.* **2012**, *134*, 154−157. (c) Janin, M.; Ghilane, J.; Lacroix, J.-C. *J. Am. Chem. Soc.* **2013**, *135*, 2108−2111.
(4) Facchetti, A.; Mushrush, M.; Yoon, M.H.; Hutchison, G.R.; Ratner, M.A; Marks, T.J. *J. Am. Chem. Soc.* **2004**, *126*, 13859−13874.
(5) Meng, H.; Bendikov, M.; Mitchell, G.; Helgeson, R.; Wudl, F.; Bao, Z.; Siegrist, T.; Kloc, C.; Chen, C.-H. *Adv. Mater.* **2003**, *15*, 1090.
(6) Descamps, E.; Leichle, T.; Corso, B.; Laurent, S.; Mailley, P.; Nicu, L.; Livache, T.; Bergaud, C. *Adv. Mater.* **2007**, *19*, 1816.
(7) Xu, L.; Chen, W.; Mulchandani, A.; Yan, Y. *Angew. Chem., Int. Ed.* **2005**, *44*, 6009−6012.
(8) Hermelin, E.; Petitjean, J.; Lacroix, J.-C.; Chane-Ching, K.I.; Tanguy, J.; Lacaze, P.-C. *Chem. Mater.* **2008**, *20*, 4447−4456.
(9) Wang, X.; Berggren, M.; Inganäs, O. *Langmuir* **2008**, *24*, 5942−5948.
(10) (a) Petitjean, J.; Aeiyach, S.; Lacroix, J. C.; Lacaze, P. C. *J. Electroanal. Chem.* **1999**, *478*, 92−100. (b) Meneguzzi, A.; Pham, M. C.; Lacroix, J. C.; Piro, B.; Adenier, A.; Ferreira, C. A.; Lacaze, P. C. *J. Electrochem. Soc.* **2001**, *148*, B121−B126. (c) Meneguzzi, A.; Pham, M. C.; Ferreira, C. A.; Lacroix, J. C.; Aeiyach, S.; Lacaze, P. C. *Synth Met.* **1999**, *102*, 1390−1391.
(11) (a) Rohwerder, M.; Michalik, A. *Electrochim. Acta* **2007**, *53*, 1300−1313. (b) Wessling, B.; Posdorfer, J. *Electrochim. Acta* **1999**, *44* (12), 2139. (c) Tallmann, D. E.; Spinks, G.; Dominis, A.; Wallace, G. G. *J. Solid State Electrochem.* **2002**, *6*, 73−84.
(12) Fenelon, A.; Breslin, C.B. *Electrochim. Acta* **2002**, *47*, 4467−4476.
(13) (a) Pournaghi-Azar, M.H.; Nahalparvari, H. *Electrochim. Acta* **2005**, *50*, 2107−2115. (b) Petitjean, J.; Tanguy, J.; Lacroix, J. C.; Chane-Ching, K. I.; Aeiyach, S.; Delamar, M.; Lacaze, P. C. *J. Electroanal. Chem.* **2005**, *581*, 111−121.
(14) (a) Fenelon, A.M.; Breslin, C.B. *J. Electrochem. Soc.* **2005**, *152*, D6−D11. (b) Camalet, J. L.; Lacroix, J. C.; Nguyen, T. D.; Aeiyach, S.; Pham, M. C.; Petitjean, J.; Lacaze, P. C. *J. Electroanal. Chem.* **2000**, *485*, 13−20.
(15) Biallozor, S.; Kupniewska, A. *Synth. Met.* **2005**, *155*, 443−449.
(16) Lacaze, P.C.; Lacroix, J.C.; Ghilane, J.; Randriamahazaka, H. *Electroactive conductive polymers for the protection of metal against corrosion: from micro to nano-structured films in nano-structured conductive polymers*; Eftekhari, A., Ed.; Wiley: Chichester, U.K., 2010; Chapter 16, p 631.
(17) Bazzaoui, M.; Martins, L.; Bazzaoui, E. A.; Martins, J. I. *Electrochim. Acta* **2002**, *47*, 2953−2962.
(18) Herrasti, P.; Diaz, L.; Ocon, P.; Ibanez, A.; Fatos, E. *Electrochim. Acta* **2004**, *49*, 3693.
(19) Hien, N. T. L.; Barcia, B.; Pailleret, A.; Deslouis, C. *Electrochim. Acta* **2005**, *50*, 1747−1755.
(20) Dos Santos, L. M. M.; Lacroix, J. C.; Chane-Ching, K. I.; Adenier, A.; Abrantes, L. M.; Lacaze, P. C. *J. Electroanal. Chem.* **2006**, *587*, 67−78.
(21) Fenelon, A.; Breslin, C. B. *J. Electrochem. Soc.* **2003**, *150*, B540−B546.
(22) He, J.; Tallman, D. E.; Bierwagen, G. P. *J. Electrochem. Soc.* **2004**, *151*, B644−B651.
(23) Forzani, E. S.; Zhang, H. Q.; Nagahara, L. A.; Amlani, I.; Tsui, R.; Tao, N. *Nano Lett.* **2004**, *4*, 1785−1788.
(24) Wang, Y.; Liu, J. L.; Tran, H. D.; Mecklenburg, M.; Guan, X. N.; Stieg, A. Z.; Regan, B. C.; Martin, D. C.; Kaner, R. B. *J. Amer. Chem. Soc.* **2012**, *134*, 9251−9252.
(25) (a) Qu, L. T.; Shi, G. Q. *J. Polym. Sci., Part A: Polym. Chem.* **2004**, *42*, 3170−3177. (b) Qu, L. T.; Shi, G. Q.; Yuan, J. Y.; Han, G.; Chen, F. *J. Electroanal. Chem.* **2004**, *561*, 149−156. (c) Debiemme-Chouvy, C. *Electrochem.Commun.* **2009**, *11*, 298−301. (d) Demoustier-Champagne, S.; Stavaux, P.-Y. *Chem. Mater.* **1999**, *11*, 829−834. (e) Qu, M. N.; Zhao, G. Y.; Cao, X. P.; Zhang, J. Y. *Langmuir* **2008**, *24*, 4185−4189.
(26) Li, C.; Bai, H.; Shi, G. *Chem. Soc. Rev.* **2009**, *38*, 2397−2409.

(27) (a) Hulteen, J. C.; Van Duyne, R. P. *J. Vac. Sci. Technol. A* **1995**, *13*, 1553−1558. (b) Ye, X.; Qi, L. *Nano Today* **2011**, *6*, 608−631.
(28) Sumida, T.; Wada, Y.; Kitamura, T.; Yanagida, S. *Chem. Commun.* **2000**, *17*, 1613−1614.
(29) Bartlett, P. N.; Birkin, P. R.; Ghanem, M. A.; Toh, C. S. *J. Mater. Chem.* **2001**, *11*, 849−853.
(30) Santos, L.; Martin, P.; Ghilane, J.; Lacaze, P. C.; Randriamahazaka, H.; Abrantes, L. M.; Lacroix, J. C. *Electrochem. Commun.* **2010**, *12*, 872−875.
(31) (a) Maldonado, S.; Smith, T. J.; Williams, R. D.; Morin, S.; Barton, E.; Stevenson, K. *Langmuir* **2006**, *22*, 2884−2891. (b) Corgier, B. P.; Bélanger, D. *Langmuir* **2008**, *26*, 5991−5997. (c) Santos, L.; Ghilane, J.; Lacroix, J. C. *Electrochem. Commun.* **2012**, *18*, 20−23. (d) Cernat, A.; Griveau, S.; Martin, P.; Lacroix, J. C.; Farcau, C.; Sandulescu, R.; Bedioui, F. *Electrochem. Commun.* **2012**, *23*, 141−144.
(32) Tian, S.; Wang, J.; Jonas, U.; Knoll, W. *Chem. Mater.* **2005**, *17*, 5726−5730.
(33) Lupu, A.; Lisboa, P.; Valsesia, A.; Colpo, P.; Rossi, F. *Sens. Actuators, B* **2009**, *137*, 56−61.
(34) Li, H.; Wu, N. *Nanotechnology* **2008**, *19*, 275301.
(35) Han, S. B.; Briseno, A. L.; Shi, X. Y.; Mah, D. A.; Zhou, F. M. *J. Phys. Chem. B* **2002**, *106*, 6465−6472.
(36) Yang, X.; Jin, Y.; Zhu, Y.; Tang, L.; Li, C. *J. Electrochem. Soc.* **2008**, *155*, J23−J25.
(37) Kazimierska, E.; Smyth, M.; Killard, A. *Electrochim. Acta* **2007**, *54*, 7260−7267.
(38) Norris, D. J.; Vlasov, Y. A. *Adv. Mater.* **2001**, *13*, 371−376.
(39) Shkunov, M. N.; Vardeny, Z. V.; DeLong, M. C.; Polson, R. C.; Zakhidov, A. A.; Baughman, R. H. *Adv. Funct. Mater.* **2002**, *12*, 21−26.
(40) Schwartz, B. J.; Nguyen, T.-Q.; Wu, J.; Tolbert, S. H. *Synth. Met.* **2001**, *116*, 35−40.
(41) Landfester, K.; Montenegro, R.; Scherf, U.; Guntner, R.; Asawpirom, U.; Patil, S.; Neher, D.; Kietzke, T. *Adv. Mater.* **2002**, *14*, 651−655.
(42) Xu, L.; Wang, J.; Song, Y.; Jiang, L. *Chem. Mater.* **2008**, *20*, 3554−3556.
(43) (a) Chang, K. C.; Lu, H. I.; Peng, C. W.; Lai, M. C.; Hsu, S. C.; Hsu, M. H.; Tsai, Y. K.; Chang, C. H.; Hung, W. I.; Wei, Y.; Yeh, J. M. *ACS Appl. Mater. Interfaces* **2013**, *5*, 1460−1467. (b) Weng, C. J.; Chang, C. H.; Peng, C. W.; Chen, S. W.; Yeh, J. M.; Hsu, C. L.; Wei, Y. *Chem. Mater.* **2011**, *23*, 2075−2083.
(44) De Leon, A. C. C.; Pernites, R. B.; Advincula, R. C. *ACS Appl. Mater. Interfaces* **2012**, *4*, 3169−3176.
(45) Roux, S.; Audebert, P.; Pagetti, J.; Roche, M. *J. Mater. Chem.* **2001**, *11*, 3360−3366.
(46) Cascalheira, A. C.; Abrantes, L. M. *Electrochim. Acta* **2004**, *49*, 5023−5028.
(47) Cascalheira, A. C.; Aeiyach, S.; Aubard, J.; Lacaze, P. C.; Abrantes, L. M. *Russ. J. Electrochem.* **2004**, *40*, 294−298.
(48) Wenzel, T. N. *J. Phys. Colloid Chem.* **1949**, *53*, 1466.
(49) Cassie, A. B. D. *Discuss. Faraday Soc.* **1948**, *3*, 11−16.
(50) Abdelsalam, M. E.; Bartlett, P. N.; Kelf, T.; Baumberg, J. *Langmuir* **2005**, *21*, 1753−1757.
(51) Henderson, M. J.; French, H.; Hillman, A. R.; Vieil, E. *Electrochem. Solid-State Lett.* **1999**, *2*, 631−633.